Ab initio calculations for the elastic properties of magnesium under pressure

G. V. Sin'ko* and N. A. Smirnov
Russian Federal Nuclear Center–Institute of Technical Physics, 456770 Snezhinsk, Russia
(Received 27 April 2009; revised manuscript received 24 August 2009; published 24 September 2009)

Results of *ab initio* calculations of the elastic constants for the hcp, bcc, double hcp (dhcp), and fcc magnesium in a wide range of pressures are presented. The calculated elastic constants are compared with available experimental and theoretical data. We discuss the effect of the electron topological transition that occurs when the hcp structure is compressed on results of calculations and consider possibility of observing the hcp→dhcp transition on the magnesium Hugoniot.

DOI: 10.1103/PhysRevB.80.104113 PACS number(s): 62.20.dq, 62.50.−p

I. INTRODUCTION

At present, various properties of single-crystal and polycrystalline magnesium under ambient pressure have been studied experimentally in rather detail. In particular, the elastic constants of single-crystal magnesium were measured at temperatures 4.2–300 K (Ref. 1) and their pressure derivatives were measured at room temperature.[2,3] Available are: data on shock[4,5] and static[6–8] compressibility of magnesium crystals; the melting curve is determined to 90 GPa;[9–11] the structural hcp→bcc transition at room temperature and 50 GPa (Ref. 12) which was predicted in the theoretical works[13,14] is experimentally observed. Several attempts were made to theoretically determine the phase diagram in the assumption that it included hcp, bcc, and liquid magnesium.[15–19]

Improved diamond anvil techniques enabled experiments to investigate structural transformations in crystals under pressure at temperatures much higher than room temperature. The authors of Ref. 20 experimentally studied the equation of state and structural transformations in magnesium crystals at pressures to 18.6 GPa and temperatures to 1527 K. At pressures above 9 GPa and temperatures above 1000 K they observed the structural hcp→dhcp transition that could not be observed and theoretically considered earlier. The pressures and temperatures at which melting was observed were in good agreement with available experimental and theoretical results. The existence of the dhcp structure in magnesium was also indirectly indicated in the experiment[21] which showed an anomalous broadening and splitting of the optical phonon mode E_{2g} in the Γ point at pressures 15–50 GPa and room temperature. The author of Ref. 21 believes that this feature in the phonon spectrum of magnesium may be related to the structural hcp→dhcp transition. Earlier the possible existence of the dhcp structure in compressed magnesium was also noted in the experiment.[7]

This work was stimulated by our desire to investigate the properties of different crystalline structures of magnesium because of practical interest in the best possible description of its thermodynamic properties. We investigate electronic, elastic and some thermodynamic properties of hcp, bcc, dhcp, and fcc magnesium in a wide range of pressures with the *ab initio* method FP-LMTO.[22–24]

II. CALCULATION METHOD

The dependence of energy on volume and unit cell shape was calculated using the full potential linear muffin-tin orbital (FPLMTO) method.[22] Our electron structure calculations were done for compressions ϱ/ϱ_0 from 0.909 to 2 at $T=0$ K. Hereinafter $\varrho_0=1/V_0$ is magnesium density at ambient pressure and $T=0$ K, and $V_0=154.487$ a.u. is the experimental volume at $P=0$, $T=0$ K from data on the thermal expansion of magnesium.[25] For hexagonal phases (hcp, dhcp), the equilibrium value of the lattice parameter c/a was found from the condition of energy minimum as a function of c/a at constant volume. Pressure was determined through the numerical differentiation of energy as a function of volume.

Elastic constants were calculated from the second derivatives of the specific energy with respect to chosen strains for several types of distortion. The position of atoms was optimized for all deformations in accordance with the existing degrees of freedom. A detailed description of the method we used here to calculate elastic constants under pressure can be found in Ref. 26. The thermal motion of nuclei was considered with the modified Debye model described in Ref. 23. In this model the contribution of thermal motion of nuclei to thermodynamic functions is expressed with only one parameter Θ_D—Debye temperature that is defined by elastic constants and only dependent on volume. The contribution from the thermal excitation of electrons was considered in accordance with perturbation theory.

In order to correctly compare the thermodynamic potentials of different crystalline structures and accurately determine elastic constants, the numerical error of the calculated energy must be lower than 0.1 mRy/atom. A number of tentative calculations were done to select some basic parameters of the method[22] that ensure such an error in the energy of magnesium. As a result, these parameters of the FPLMTO method were selected to be as follows. Electrons in the 1*s* state were taken as core electrons and electrons which occupied 2*s*, 2*p*, and 3*s* states in the isolated atom were taken as valence electrons. In spherical harmonic expansions, the parameters of the method[22] are as follows: $l^b_{\max}=2$ in the wave function representation, $l^w_{\max}=6$ in the potential and charge density expansion, and $l^\tau_{\max}=12$ in the Hankel function reexpansion in the Bessel functions. The *d*-type orbitals are present in the basis because these states are of no small effect on energy. We used ten centers of linearization and four energy tails that were selected in accordance with the algorithm proposed in Ref. 24.

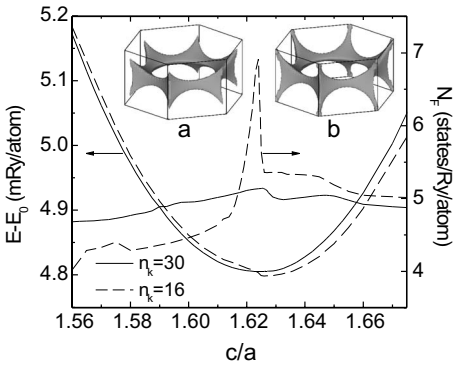

FIG. 1. Calculated energy and density of states on the Fermi level versus c/a for hcp magnesium at $n_k=16$ and 30. $\varrho/\varrho_0=1.1765$, $E_0=-401.161$ Ry/atom. The Fermi surfaces a and b correspond to the second valence band.

The mesh for integration in reciprocal space with the linear tetrahedron method was constructed in the prism-shaped Brillouin zone by dividing each edge into the same number of parts n_k. We gave special attention to the selection of this parameter defining the number of $\vec{k}$ points to be used in calculations. As mentioned earlier in Refs. 27 and 28 the accuracy of determining the parameter c/a and elastic constants under pressure is strongly dependent on the mesh fineness in the Brillouin zone. In particular, this is related to the electron topological transitions (ETT) that occur in crystals under pressure.[28] As a result, we found an ETT in hcp magnesium, which occurred under compression and influenced on calculated results. We also determined an acceptable value of n_k that helped minimize that influence. Figure 1 shows energy and density of state on the Fermi surface versus c/a for different numbers of $\vec{k}$ points at $\varrho/\varrho_0=1.1765$ ($\approx$7.7 GPa). It is seen that at $n_k=16$ the dependence $E(c/a)$ has a break near the minimum and the density of states on the Fermi level has a characteristic peak which corresponds to the ETT shown in the insert of Fig. 1 (surfaces a and b). The ETT occurs in the second valence band. If increase n_k to 30, then, as seen in Fig. 1, the effect of the ETT on $E(c/a)$ becomes much weaker and the peak in the density of states becomes much lower.

To see how the ETT influences on the pressure dependence of elastic constants at different meshes in the $\vec{k}$ space, consider deformation of hcp lattice in the parameter c/a.

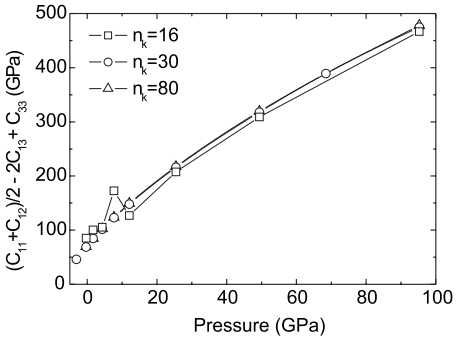

FIG. 2. The pressure dependence of the combination of elastic constants $C(P)$ for hcp magnesium at $n_k=16$, 30 and 80.

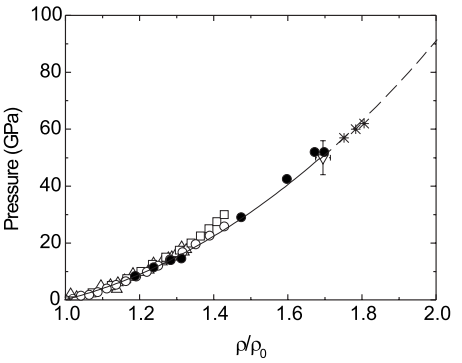

FIG. 3. Calculated pressure versus compression for hcp (solid) and bcc (dashed) magnesium on the isotherm $T=300$ K in comparison with experimental results at room temperature: ▽—the point of the hcp→bcc transition, (Ref. 12) ●—hcp magnesium (Ref. 32), *—bcc magnesium, (Ref. 32), □ (Ref. 6), ○ (Ref. 7), and △ (Ref. 20).

This deformation defines the following combination of elastic constants:[26]

$$C(P) = (C_{11} + C_{12})/2 - 2C_{13} + C_{33}.$$

We calculated $C(P)$ for $n_k=16$, 30 and 80. Obtained results are shown in Fig. 2. It is clearly seen that $C(P)$ is not smooth at $n_k=16$. In this case, near $P\approx7.7$ GPa, where the ETT occurs in the unstrained crystal, the curve $C(P)$ starts to oscillate. The break of the curve $E(c/a)$ makes the calculated elastic constants be strongly dependent on the method used to approximate calculated results. When n_k is increased to 30, oscillations disappear and $C(P)$ becomes smooth and this corresponds to $E(c/a)$ with no break. The further increase of n_k changes the elastic constants by no more than 1%.

Thus, in integration over the Brillouin zone in the $\vec{k}$ space, the value of the parameter n_k defining the mesh in the space, was taken to be 30. As a result, the irreducible part of the Brillouin zone in the case of the hcp structure was found to

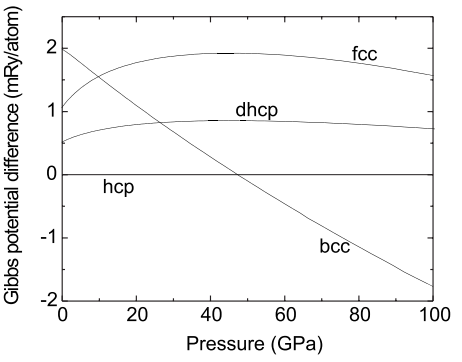

FIG. 4. Gibbs potential difference versus pressure for hcp, bcc, dhcp, and fcc magnesium at $T=0$ K, plotted relative to the Gibbs potential of the hcp structure.

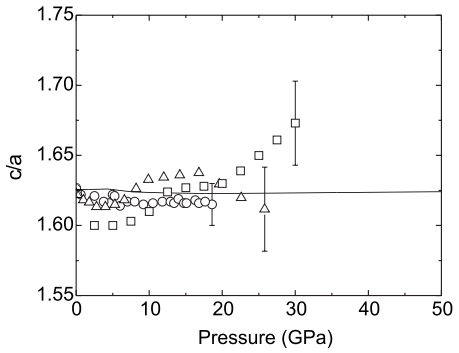

FIG. 5. c/a versus pressure at $T=0$ K for hcp magnesium in comparison with experimental data at room temperature. The line shows the calculation and the symbols show experimental data: ○,(Ref. 20) □ (Ref. 6), and △ (Ref. 7).

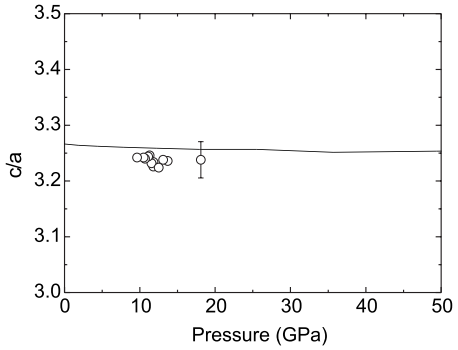

FIG. 6. c/a versus pressure at $T=0$ K for dhcp magnesium in comparison with experimental data at temperatures from 1127 to 1477 K. The line shows the calculation and ○-experimental data from. (Ref. 20)

contain 1456 $\vec{k}$ points. Our studies showed that for the other structures of interest, $n_k=30$ was also sufficient to perform calculations with required accuracy. In calculations we took into account the Blochl corrections.[29]

The choice of form for exchange-correlation energy is of an appreciable effect on calculated results. In the literature there are several approximations for the local exchange-correlation functional (XC). To this functional gradient corrections can be added. The choice of XC is important because it is impossible to choose from among the existing expressions the best one for all materials since the use of one and the same approximation of exchange-correlation energy for different materials results in different accuracy. To choose the best XC for magnesium, we, for its hcp structure, calculated the equilibrium volume V_0, bulk modulus B_0, and its pressure derivative B_0' for different XC and then compared them with experimental results. As a result, we decided to do further calculations with the Barth-Hedin functional[30] together with gradient corrections.[31] This potential gives good agreement with the experiment.

III. CALCULATED RESULTS

To judge about the accuracy of our calculations we compared them with available experimental data. Figure 3 shows the calculated isotherm $T=300$ K with account for the hcp→bcc transition along with experimental data. The thermal motion of nuclei was considered on the basis of the modified Debye model.[23] The calculated curve is seen to agree well with experiment. The values of V_0, B_0, and B_0' at $T=300$ K were calculated to be, respectively, 156.84 a.u., 33 GPa, and 4.32 which is also in agreement with experimental data.

Using the calculated energies and pressures, we found the Gibbs potentials $G=E+PV$ of magnesium structures under study versus pressure at zero temperature. Figure 4 shows these potentials plotted relative to the Gibbs potential of hcp magnesium. Our calculations show that the hcp structure is the most stable at ambient pressure which is in agreement with experiment. The increase of pressure at $T=0$ K causes the transition from hcp to bcc. The pressure of the transition is 47.3 GPa which agrees well with the experiment,[12] where the pressure was observed to be 50 ± 6 GPa at room temperature. In our calculation the change of volume in the hcp→bcc transition is 0.6%. This is also in good agreement with ≈1% reported in.[12] It is seen from Fig. 4 that neither the dhcp, nor the fcc structure becomes most favorable in the pressure range under study at $T=0$ K.

We also compared the calculated pressure dependence of c/a with experiment. Figure 5 shows the calculated $c/a(P)$ for hcp magnesium along with experimental data at room temperature. They seem to agree well. The calculated value of c/a at $P=0$ is 1.626 and the corresponding measured value varies from 1.623 to 1.626.[6,7,20]

Figure 6 shows the calculated $c/a(P)$ for hhcp magnesium and experimental data at high temperature.[20] They also seem to agree well. Apparently the effect of temperature on this parameter is small. Our calculations show that the effect of pressure on it is small, too.

Consider next the accuracy of calculated elastic constants. Table I contains elastic constants calculated in this work and

TABLE I. Calculated elastic constants (in GPa) for hcp magnesium at $P=0$, $T=0$ K in comparison with experimental data.

	C_{11}	C_{33}	C_{44}	C_{66}	C_{12}	C_{13}	G
Our calculation	63.44	68.47	18.32	18.65	26.15	21.07	19.4
Calculation[33]	60.77	65.35	15.32	17.37	31.36	20.97	16.4
Experiment[1]	63.48	66.45	18.42	18.75	25.94	21.70	19.8

TABLE II. Calculated pressure derivatives of elastic constants and shear module for hcp magnesium at $P=0$ and $T=0$ K and experimental results at room temperature.

	$\frac{\partial C_{11}}{\partial P}$	$\frac{\partial C_{33}}{\partial P}$	$\frac{\partial C_{44}}{\partial P}$	$\frac{\partial C_{66}}{\partial P}$	$\frac{\partial G}{\partial P}$
Calculation	6.414	7.250	1.628	1.331	1.65
Experiment[2]	6.23	7.29	1.60	1.37	
Experiment[3]	6.13	7.22	1.58	1.36	
Experiment[36]					1.70

in Ref. 33 (GGA calculation) at zero pressure and temperature and experimental results extrapolated to $T=0$ K. It is seen that first, our results excellently agree with experiment; the error does not exceed 3%. Second, our calculations satisfactorily agree with calculations from;[33] the maximal deviation is about 20%. Much higher accuracy in our determination of elastic constants comes from our thorough selection of the inner parameters of our calculation method. Table I also contains values of the shear modulus G for the hcp polycrystal; $G=(G_V+G_R)/2$, where G_V and G_R are shear moduli averaged according to Voigt and Reuss.[34,35] Our value of G is seen to agree well with experiment. Using the dependences of elastic constants on pressure obtained in this work, we calculated their pressure derivatives $\partial C_{ij}/\partial P$ at $P=0$. In Table II they are compared with experimental data for hcp magnesium. The calculated derivatives are seen to differ from experimental values by no more than 5%. This suggests that our elastic constants versus pressure are calculated at high accuracy. Table II also contains the calculated and experimental value of shear modulus derivative for the polycrystal $\partial G/\partial P$; it is seen to agree well, too.

Having seen that our calculations are highly accurate, turn now to the results of the magnesium elastic constants calculation at ϱ from 0.909, ϱ_0 to 2 ϱ_0 at $T=0$ K. Their values for hcp, dhcp, bcc, and fcc magnesium versus relative volume are provided in Tables III and IV.

We compared our pressure dependences of elastic constant for hcp magnesium with those calculated in the LDA approximation.[37] Figure 7 demonstrates the result of this comparison. With account for the different calculation methods and forms of the exchange-correlation potentials one can admit that the results satisfactorily agree. Unlike the elastic constants obtained in Ref. 37 our ones vary smoothly, including in the region ~10 GPa where the ETT mentioned shows itself. Unphysical oscillations due to calculation errors in the ETT region are especially well seen on the curve constructed from results obtained in Ref. 37 for the elastic constant $C_{66}=(C_{11}-C_{12})/2$.

In Ref. 38 the pressure dependences of shear modulus for hcp and bcc magnesium at $T=300$ K were calculated with use of generalized pseudopotential theory. We also calculated them for hcp, bcc, and dhcp magnesium, but at $T=0$ K. Figure 8 shows our results and results from Ref. 38. With account for the different temperatures it is seen that the compared values of $G(P)$ agree quite well. The difference is no

TABLE III. Calculated elastic constants of hcp and dhcp magnesium at $T=0$ K (in GPa).

ϱ_0/ϱ	C_{11}	C_{12}	C_{13}	C_{33}	C_{44}
			hcp structure		
1.10	42.500	14.798	13.015	43.316	12.695
1.00	61.375	24.962	20.370	66.348	17.873
0.90	89.188	42.408	30.341	96.348	24.442
0.80	126.88	69.488	46.791	143.41	33.261
0.70	182.97	114.72	73.776	214.73	44.668
0.60	267.54	193.10	122.11	331.72	58.952
0.55	326.87	254.11	160.79	420.28	68.136
0.50	402.26	344.05	215.84	533.46	74.928
			dhcp structure		
1.10	41.845	14.447	13.030	44.929	12.235
1.00	60.139	25.870	20.136	67.409	16.837
0.80	127.23	71.835	46.047	143.70	29.421
0.70	180.80	118.05	72.629	214.03	36.534
0.60	257.72	203.25	120.77	329.65	48.255
0.55	312.41	268.47	159.34	416.29	57.020
0.50	385.01	362.33	213.06	527.17	64.362

TABLE IV. Calculated elastic constants of bcc and fcc magnesium at $T=0$ K (in GPa).

ϱ_0/ϱ	C_{11}	C_{12}	C_{44}
bcc structure			
1.10	20.896	22.849	22.029
1.00	34.277	34.303	31.499
0.90	54.869	50.574	43.604
0.80	86.137	74.921	61.285
0.70	136.51	112.29	84.626
0.60	217.38	176.36	116.80
0.55	277.49	226.13	136.40
0.50	359.78	293.74	159.05
fcc structure			
1.10	31.061	19.652	175.11
1.00	44.092	31.409	252.02
0.90	61.565	49.241	373.41
0.80	86.177	76.676	533.50
0.70	120.95	122.31	767.26
0.60	181.79	196.30	1116.7
0.50	289.50	329.34	1647.6

higher than 7%. The curves shown in Fig. 8 for the hcp and dhcp structures are nonmonotone. Both the structures under pressure tend to softening, and the dhcp to a greater extent.

Our calculations show that the bcc structure is mechanically unstable at $T=0$ and low pressures ($P<10$ GPa). This is in agreement with calculations done with generalized pseudopotential theory[18,38] and phonon spectrum calculations for bcc magnesium.[19] And vice versa, fcc at $T=0$ K is mechanically unstable at high pressure ($P>20$ GPa).

We have also calculated three Higoniots: the first in the assumption that the hcp structure does not change in compression; the second in the assumption that the hcp→bcc transition occurs on the Hugoniot; and the third in the assumptions that the hcp→dhcp transition occurs on the Hugoniot. Figure 9 shows the results we obtained and experimental data.[4,5] It is seen from the figure that at pressures $P>35$ GPa experimental data are closest to the Hugoniot

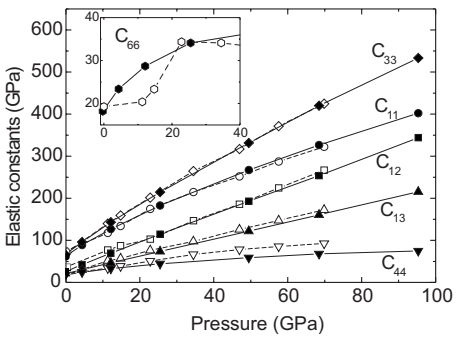

FIG. 7. Elastic constants versus pressure at $T=0$ K for hcp magnesium. Filled symbols show our results and unfilled ones show data from. (Ref. 37)

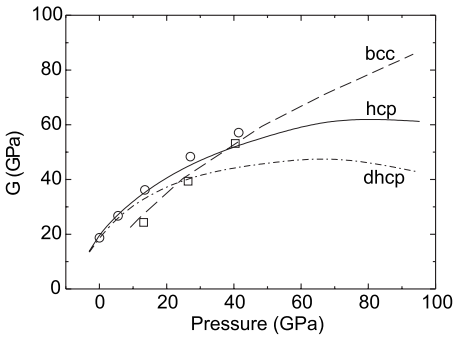

FIG. 8. Shear modulus G versus pressure for polycrystalline magnesium. The lines show our results at $T=0$ K. The symbols show results from Ref. 38 at $T=300$ K: ○ hcp, □ bcc.

section that corresponds to the bcc structure. On the other hand, the position of the experimentally found[20] interface between the hcp and dhcp phases (see Fig. 10) suggests that the dhcp structure can appear on the Hugoniot if only $P>20$ GPa.

Thus, we may assume that if the Hugoniot crosses the region where the dhcp phase exists, this occurs within a relatively narrow range of pressures $20<P<35$ GPa where all the three curves shown in Fig. 9 practically coincide. The bcc phase is stable above and the hcp phase is stable below this range of pressures. Additional experiments and calculations are needed to determine the proper position of the dhcp structure on the phase diagram. In particular, the experimental measurement of sound velocity behind a shock wave front may be useful. Our estimates suggest that the measurement of the transverse sound velocity is more promising. So, during the hcp→dhcp transition the transverse sound velocity is expected to change by ~7%, while the longitudinal one will change by no more than 2.5%.

IV. CONCLUSION

Using *ab initio* calculations, we have investigated the behavior of different magnesium structural modifications under

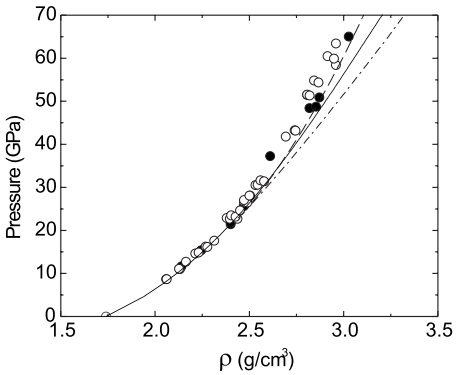

FIG. 9. Magnesium Hugoniot on (P,ϱ) plane. Our results are shown by lines: the solid is for the hcp structure, the dashed is with the hcp→bcc transition, and the dotted-and-dashed is with the hcp→dhcp transition. Symbols show data from shock experiments: ○ (Ref. 5) and ● (Ref. 4).

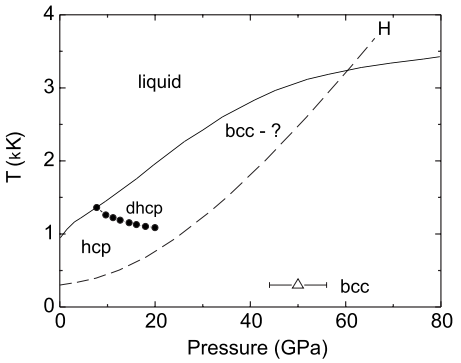

FIG. 10. Lines on magnesium phase diagram. ● hcp–dhcp interface (Ref. 20), — - melting curve (Ref. 9), – – - Hugoniot (Ref. 4), △ the point of the hcp→bcc transition at room temperature. (Ref. 12)

pressure. The elastic and thermodynamic properties of hcp, dhcp, bcc, and fcc magnesium under pressure were determined. We considered the question concerning the accuracy of the elastic constants C_{ij} we calculated and the effect of the electron topological transition on accuracy. It was shown that the effect of the isolated ETT on the accuracy of calculation C_{ij} could be done insignificant by taking a large enough number of $\vec{k}$ points in the Brillouin zone. Our pressure dependences of c/a, elastic constants, and polycrystalline shear moduli for magnesium structures under study agree well with available experimental data and data from other calculations. The estimate of the sound velocity changing behind the shock front due to the structural hcp→dhcp transition are presented.

ACKNOWLEDGMENT

This work was supported by the Russian Foundation for Basic Research (Grant No. 08-08-01055).

*gevas@uniterra.ru

[1] L. J. Slutsky and C. W. Garland, Phys. Rev. **107**, 972 (1957).
[2] E. R. Naimon, Phys. Rev. B **4**, 4291 (1971).
[3] R. E. Schmunk and C. S. Smith, J. Phys. Chem. Solids **9**, 100 (1959).
[4] R. F. Trunin, L. F. Gudarenko, M. F. Zhernokletov, and G. V. Simakov, *Experimental Data on Shock Compression and Adiabatic Expansion of Condensed Matter* (Sarov: Russian Federal Nuclear Center–Institute of Experimental Physics, 2006), p. 92.
[5] *Los Alamos Shock Hugoniot Data*, edited by S. P. Marsh (University of California Press, Berkeley, CA, 1980).
[6] G. L. Clendenen and H. G. Drickamer, Phys. Rev. **135**, A1643 (1964).
[7] E. A. Perez-Albuerne, R. L. Clendenen, R. W. Lynch, and H. G. Drickamer, Phys. Rev. **142**, 392 (1966).
[8] H. Olijnyk and W. B. Holzapfel, Phys. Lett. **100A**, 191 (1984).
[9] P. A. Urtiew and R. J. Grover, J. Appl. Phys. **48**, 1122 (1977).
[10] G. C. Kennedy and R. C. Newton, in *Solids Under Pressure*, edited by W. Paul and D. M. Warschauer (McGraw-Hill, New York, 1963), p. 163.
[11] D. Errandonea, R. Boehler, and M. Ross, Phys. Rev. B **65**, 012108 (2001).
[12] H. Olijnyk and W. B. Holzapfel, Phys. Rev. B **31**, 4682 (1985).
[13] J. A. Moriarty and A. K. McMahan, Phys. Rev. Lett. **48**, 809 (1982).
[14] A. K. McMahan and J. A. Moriarty, Phys. Rev. B **27**, 3235 (1983).
[15] J. L. Pelissier, Phys. Scr. **34**, 838 (1986).
[16] R. M. Wentzcovitch and M. L. Cohen, Phys. Rev. B **37**, 5571 (1988).
[17] J. D. Althoff, P. B. Allen, R. M. Wentzcovitch, and J. A. Moriarty, Phys. Rev. B **48**, 13253 (1993).
[18] J. A. Moriarty and J. D. Althoff, Phys. Rev. B **51**, 5609 (1995).
[19] S. Mehta, G. D. Price, and D. Alfe, J. Chem. Phys. **125**, 194507 (2006).
[20] D. Errandonea, Y. Meng, D. Hausserman, and T. Uchida, J. Phys.: Condens. Matter **15**, 1277 (2003).
[21] H. Olijnyk, J. Phys.: Condens. Matter **11**, 6589 (1999).
[22] S. Yu. Savrasov and D. Yu. Savrasov, Phys. Rev. B **46**, 12181 (1992).
[23] G. V. Sin'ko and N. A. Smirnov, J. Phys.: Condens. Matter **14**, 6989 (2002).
[24] G. V. Sin'ko and N. A. Smirnov, Phys. Rev. B **74**, 134113 (2006).
[25] S. I. Novikova, *Thermal Expansion of Solids* (Nauka, Moscow, 1974).
[26] G. V. Sin'ko, Phys. Rev. B **77**, 104118 (2008).
[27] G. Steinle-Neumann, L. Stixrude, and R. E. Cohen, Phys. Rev. B **63**, 054103 (2001).
[28] G. V. Sin'ko and N. A. Smirnov, J. Phys.: Condens. Matter **17**, 559 (2005).
[29] P. E. Blochl, O. Jepsen, and O. K. Andersen, Phys. Rev. B **49**, 16223 (1994).
[30] U. von Barth and L. Hedin, J. Phys. C **5**, 1629 (1972).
[31] J. P. Perdew, J. A. Chevary, S. H. Vosko, K. A. Jackson, M. R. Pederson, D. J. Singh, and C. Fiolhais, Phys. Rev. B **46**, 6671 (1992); **48**, 4978(E) (1993).
[32] H. Olijnyk, J. Phys.: Condens. Matter **16**, 8791 (2004).
[33] F. Jona and P. M. Marcus, Phys. Rev. B **66**, 094104 (2002).
[34] W. Voigt, *Lehrbuch der Krystall Physik* (Teubner, Leipzig, 1928), p. 962.
[35] A. Reuss, Z. Angew. Math. Mech. **9**, 49 (1929).
[36] M. Guinan and D. Steinberg, J. Phys. Chem. Solids **35**, 1501 (1974).
[37] F. Jona and P. M. Marcus, J. Phys.: Condens. Matter **15**, 7727 (2003).
[38] C. W. Greeff and John A. Moriarty, Phys. Rev. B **59**, 3427 (1999).